Clays and Clay Minerals, Vol. 51, No. 3, 318–326, 2003.

STRUCTURAL STUDY OF MAYA BLUE: TEXTURAL, THERMAL AND SOLID-STATE MULTINUCLEAR MAGNETIC RESONANCE CHARACTERIZATION OF THE PALYGORSKITE-INDIGO AND SEPIOLITE-INDIGO ADDUCTS

BASIL HUBBARD, WENXING KUANG, ARVIN MOSER, GLENN A. FACEY AND CHRISTIAN DETELLIER*

Center for Catalysis Research and Innovation, Department of Chemistry, University of Ottawa, Ottawa, Ontario, Canada K1N 6N5

Abstract—Palygorskite-indigo and sepiolite-indigo adducts (2 wt.% indigo) were prepared by crushing the two compounds together in a mortar and heating the resulting mixtures at 150 and 120ºC, respectively, for 20 h. The samples were tested chemically to ensure that they displayed the characteristic properties of Maya Blue. Textural analysis revealed that no apparent changes in microporosity occurred in sepiolite or palygorskite after thermal treatment at 120ºC (sepiolite) and 150ºC (palygorskite) for 20 h. Micropore measurements showed a loss of microporosity in both sepiolite and palygorskite after reaction with indigo. The TGA-DTG curves of the sepiolite-indigo and palygorskite-indigo adducts were similar to their pure clay mineral counterparts except for an additional weight loss at ~360ºC due to indigo.

The ^{29}Si CP/MAS-NMR spectrum of the heated sepiolite-indigo adduct is very reminiscent of the spectrum of dehydrated sepiolite. Crushing indigo and sepiolite together initiates a complexation, clearly seen in the ^{13}C CP/MAS-NMR spectrum, which can be driven to completion by heat application. In contrast to the broad peaks of the pure indigo ^{13}C CP/MAS-NMR spectrum, the sepiolite-indigo adduct spectrum consists of a well-defined series of six narrow peaks in the 120.0–125.0 ppm range. In addition, the sepiolite-indigo spectrum has two narrow, shifted peaks corresponding to the carbonyl group and the C-7 (C-16) of indigo. A model is proposed in which indigo molecules are rigidly fixed to the clay mineral surface through hydrogen bonds with edge silanol groups, and these molecules act to block the nano-tunnel entrances.

Key Words—Indigo, Maya Blue, Palygorskite, Sepiolite, Solid-State Multinuclear Magnetic Resonance, Textural Analysis, Thermal Analysis.

INTRODUCTION

Merwin (1931) discovered an illustrious and remarkably resistant blue paint present on the remains of Mayan wall paintings at Chichen Itza in the Yucatan. In referring to this pigment, Gettens and Stout (1946) first employed the term "Mayan Blue" which was subsequently renamed "Maya Blue". Mayans, who inhabited Mesoamerica during the late Classical period, are reported to have started using Maya Blue on temple murals and religious effigies as early as the 6th century AD (Gettens, 1962). Archeological evidence suggests that the pigment's application to mural paintings continued in Spain during the 16th and 17th centuries and until the 19th century in Cuba under the trade name Havana Blue (Tagle *et al.*, 1990).

The predominant chemical constituents of Maya Blue were identified as the fine clay minerals palygorskite and sepiolite (Gettens, 1962). Initially, Gettens (1962) hypothesized that the pigment was purely of an inorganic nature, composed solely of a blue palygorskite mineral. Shepard (1962) introduced the idea of Maya Blue being a complex consisting of an inorganic carrier and an organic dye. Although no record of the original method of Maya Blue preparation exists, van Olphen (1966) pioneered a synthesis for a complex analogous to Maya Blue by heating indigo and palygorskite. In a comparative study by Kleber *et al.* (1967), it was found that the Fourier transform infrared (FTIR) and powder X-ray diffraction (PXRD) spectra of the synthetic palygorskite-indigo complex were roughly equivalent to the corresponding spectra obtained from authentic Maya Blue samples.

The major components of Maya Blue, palygorskite and sepiolite, are classified as fibrous phyllosilicates (Brindley, 1959; Pedro, 1972). Both consist of continuous, two-dimensional talc-like tetrahedral sheets of composition T_2O_5 (T = Si, Al, Be,....) and yet lack the conventional continuous octahedral sheets of other layer silicates. Both palygorskite and sepiolite have a 2:1 tetrahedral:octahedral framework with one 2:1 unit joined to the next by inversion of the SiO_4 tetrahedra along Si–O–Si bonds. Extending parallel to the x axis, palygorskite ribbons have an approximate width along the y axis of two linked pyroxene-like chains; sepiolite ribbons measure three linked pyroxene-like chains. The tetrahedral and octahedral mesh gives rise to a series of rectangular tunnels, which run parallel to the x axis. Palygorskite tunnels measure 6.4 × 3.7 Å when projected in the yz plane; sepiolite tunnels measure 10.6 × 3.7 Å. In addition to exchangeable cations, zeolitic (bound) water permeates these tunnels. Thermogravimetric analysis (TGA) and differential thermal analysis (DTA)

* E-mail address of corresponding author:
dete@science.uottawa.ca
DOI: 10.1346/CCMN.2003.0510308

reveal an endothermic reaction occurring at 150ºC in palygorskite and at 120ºC in sepiolite corresponding to the loss of this zeolitic water (Jones and Galán, 1998). Generally, sorption of molecules into the microporous tunnels is accomplished through hydrogen-bond interaction with the internal coordinated water of the clay mineral, after removal of zeolitic water (Serna and van Scoyoc, 1979). For example, small organic molecules such as acetone (Weir *et al.*, 2000) and pyridine (Ruiz-Hitzky, 2001) have been shown to intercalate into the microporous tunnels of sepiolite following dehydration.

On the surface of the clay minerals, broken Si–O–Si bonds compensate residual charge through protonation or hydroxylation, forming silanol (Si–OH) groups. These groups are readily reactive with molecules adsorbed on the external surfaces of the minerals. In terms of abundance, silanol and silanol-derived groups are found at regular intervals of ~5 Å parallel to the axis of the fiber of sepiolite (Ahlrichs *et al.*, 1975). The fibrous structure of palygorskite and sepiolite may be damaged through prolonged treatment with strong acid. Sepiolite is especially sensitive to strong acid due to its high magnesic component and the large size of its structural micropores (Myriam *et al.*, 1998). Recently, sepiolite has shown great promise as a material used in the production of inorganic membranes for ultrafiltration (Wang *et al.*, 2001; Weir *et al.*, 2001). It was reported that zeolite-sepiolite composite membranes might be applied effectively to several gas separation processes (Le Van Mao *et al.*, 1999).

The structure of indigo, a vat dye that may be derived naturally from sprigs of xiuquilit or produced synthetically, was first described by Von Baeyer (Cooksey and Dronsfield, 2002) who proposed a *cis*-isomer. In 1926, X-ray crystallography showed that indigo actually exists as a *trans*-isomer. Indigo, with the chemical formula $C_{16}H_{10}N_2O_2$ (Figure 1), is quasi-planar, with a slightly elongated central C=C bond and an elongated C=O bond. Hydrogen attractions between adjacent molecules cause structural bending of the molecule, as well as solid-state aggregation in which one indigo molecule is linked to four others. The aggregates are durable, and it was noted that diminished intermolecular attractions between neighboring indigo molecules remain even in vapor phase (Gordon and Gregory, 1983).

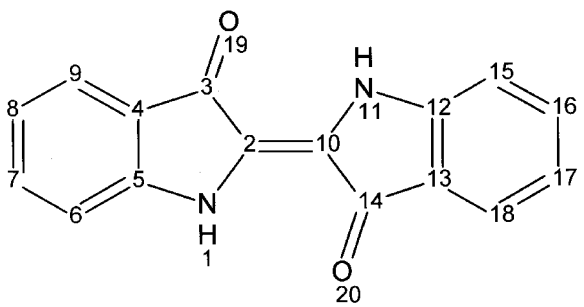

Figure 1. Structure of indigo.

The mechanism behind Maya Blue's stability in concentrated mineral acids, alkalis, organic solvents, oxidants and reducing agents has been, and remains, a widely debated polemic (Tagle *et al.*, 1990). Van Olphen (1966) suggested that the indigo molecules are too big to enter into the tunnels of palygorskite or sepiolite, and consequently are adsorbed only on the external surfaces of the clay mineral. Moreover, he proposed that the longitudinal sections found on the surface of palygorskite and sepiolite shift over the top of indigo molecules buried in external grooves, locking them in place and shielding them from acid attack. Kleber *et al.* (1967) popularized the idea of indigo molecules being intercalated inside the microporous tunnels of palygorskite.

The fascination with Maya Blue lies not only in its durability, but also in its coloration and luster. Although the dye content of Maya Blue may approach a mere 5%, the color is unusually radiant (Kleber *et al.*, 1967). In addition to identifying the superlattice structure of the pigment, Jose-Yacaman *et al.* (1996) discovered the presence of metallic and oxide nanoparticles in Maya Blue. These nanoparticles may be responsible for the brillance of the pigment (Jose-Yacaman *et al.*, 1996). Recently, X-ray absorption near edge structure (XANES), extended X-ray adsorption fine structure (EXAFS), and high-resolution transmission electron microscopy (HRTEM) have been used to further the understanding of the role of Fe and Fe nanoparticles in Maya Blue samples (Polette *et al.*, 2002).

In the present work, we studied the preparation and properties of palygorskite-indigo and sepiolite-indigo complexes through various chemical experiments. Additionally, we characterized these complexes through spectroscopic and analytical techniques including FTIR, PXRD, TGA, DTA, derivative thermogravimetric analysis (DTG), and solid-state multinuclear magnetic resonance. Textural analysis of palygorskite-indigo and sepiolite-indigo adducts was also performed, yielding quantitative data on the internal micropores of the samples. The results of our investigation indicate the presence of a strong interaction between indigo molecules and the surface bordering the clay mineral nanotunnels.

MATERIALS AND METHODS

Materials

Crude palygorskite (PFl-1) and sepiolite (SepSp-1) samples were obtained from The Clay Minerals Society's Source Clay Mineral Repository. Both samples were purified using standard procedures (Weir *et al.*, 2001) consisting of crushing and centrifuging, weak acid/base treatment (to destroy carbonates), and saturation in a saline solution (to allow Na^+ exchange to occur). Removal of the Cl^- ions (checked with $AgNO_3$) was accomplished by diffusion through dialysis tubing. The particle size of palygorskite and sepiolite clusters

https://doi.org/10.1346/CCMN.2003.0510308 Published online by Cambridge University Press

used in experimentation was selectively restricted by passing the clay mineral samples through a 100-mesh sieve, having a pore opening of 0.15 mm. Synthetic indigo (2-(1,3-dihydro-3-oxo-2H-indol-2-ylid-ene)-1,2-dihydro-3H-indol-3-one; ~95%) was obtained from Aldrich Chemical Company and used as received.

Preparation of the indigo adducts

Palygorskite-indigo complexes were prepared using a procedure adapted from one of van Olphen's experiments (van Olphen, 1966). Synthetic indigo was mixed in a mortar and pestle with a fixed proportion of purified palygorskite. Using a pestle, the heterogeneous mixture was crushed vigorously for several minutes at room temperature until it became a fine, consistent, light-blue powder. Fractions of the mixture were removed and analyzed using several spectroscopic techniques. The powder was then transferred into a glass Petri dish, and heated in a furnace at 150ºC for 20 h. Samples were heated for 20 h to ensure complete reaction of the dye with the clay mineral. Sepiolite-indigo complexes were prepared and tested in a similar manner. However, rather than heating samples at 150ºC for 20 h, samples were heated at 120ºC for 20 h, to correspond with the zeolitic water loss of sepiolite (Jones and Galán, 1998).

PXRD and FTIR

Powder XRD was performed on palygorskite-indigo and sepiolite-indigo samples using a Philips PW3710 diffractometer (CuKα, λ = 1.54186 Å). Relative transmittance spectra of the palygorskite-indigo and sepiolite-indigo complexes were acquired on a Bomem MB-100 FTIR instrument in the range 4000–400 cm^{-1} using KBr discs (0.5 mg of sample to 50 mg of KBr). Sixteen scans were taken and the resolution was 4 cm^{-1}.

Thermal analysis

The TGA, DTA and DTG analyses were performed using a SDT 2960 Simultaneous DSC-TGA instrument. Approximately 10–15 mg of sample were placed in the instrument's platinum crucible. The furnace chamber was flooded with He gas throughout the analysis operation. Although several different heating strategies were used to analyze samples, a uniform ramp rate of 10ºC/min was used.

Textural analysis

The BET surface area and micropore measurements of the samples were processed on a Micromeritics ASAP-2010 instrument (N_2 adsorption at –196ºC). The samples were pre-degassed at room temperature under vacuum to eliminate adsorbed moisture and zeolitic water within the micropores. The degas process was terminated when the vacuum pressure decreased to 3 μmHg. The molecular cross-section of nitrogen used in the data analysis was 0.1620 nm^2. The typical range of thickness chosen for t-plot measurements was 3.5 to 5 Å.

Multinuclear magnetic resonance

Cross-polarization magic-angle spinning nuclear magnetic resonance (CP/MAS-NMR) characterization was performed on both palygorskite-indigo and sepiolite-indigo adducts. Several samples were analyzed on a Bruker ASX 200 spectrometer while others were studied on a Bruker Avance 500 spectrometer. The ^{29}Si spectra were acquired at 39.75 MHz on the ASX 200, and at 99.36 MHz on the Avance 500 spectrometer. The ^{13}C spectra were acquired at 50.31 MHz on the ASX 200 and at 125.75 MHz on the Avance 500. A ramped CP pulse was used in all ^{29}Si and ^{13}C cross-polarization experiments. The recycle delay time was 2 s, and the proton 90º pulse was 4 μs. The contact time to allow the transfer of magnetization between protons and $^{29}Si/^{13}C$ nuclei was 2 ms for ^{13}C and 10 ms for ^{29}Si. Typical spinning rates for ^{13}C experiments and ^{29}Si experiments were 5 and 4 kHz, respectively, on the ASX 200 spectrometer, and 14 kHz and 8 kHz, respectively, on the Avance 500. The Hartman-Hahn condition was met in all CP/MAS experiments. The ^{29}Si NMR signals were externally referenced to the $-Si(CH_3)_3$ resonance of tetrakis trimethylsilylsilane at –9.9 ppm, corresponding to tetramethylsilane (TMS) at 0 ppm. The ^{13}C signals were externally referenced to the high-frequency signal of adamantane at 38.4 ppm.

RESULTS AND DISCUSSION

Visually, laboratory preparations of the palygorskite-indigo complex (2 wt.% indigo) were light blue in color prior to thermal treatment. After heating, the samples developed a greenish color. The sepiolite-indigo mixtures were originally a light-blue color, and became darker after heating. The difference in the coloration of the samples could be due to the relatively high concentration of Fe in palygorskite (Polette *et al.*, 2002). Small representative samples were taken from the heated palygorskite-indigo and sepiolite-indigo preparations and tested to ensure that they displayed the characteristic resistance of Maya Blue to organic solvents (acetone, chloroform, methanol), acids (hydrochloric acid, sulfuric acid, nitric acid), and bases (sodium hydroxide, potassium hydroxide).

Chemical resistance of sepiolite- and palygorskite-indigo complexes

After immersing sample fractions into vials containing both cool and boiling concentrated acids, bases and organic solvents, no reducing effects in coloration were observed. Extraction of indigo with nitric acid proved to be the most easily identifiable chemical test for Maya Blue. When pure indigo, or an unheated heterogeneous mixture of palygorskite and indigo is immersed in a concentrated solution of nitric acid, the dye is immediately transformed to a yellow-red water-soluble indigoid derivative, isatin (van Olphen, 1966). Yet the indigo

https://doi.org/10.1346/CCMN.2003.0510308 Published online by Cambridge University Press

present in heated palygorskite-indigo complexes does not react with nitric acid. Moreover, it became evident during experimentation that heterogeneous well-crushed samples of sepiolite-indigo display the characteristic chemical properties of Maya Blue, such as resistance to nitric acid, without the application of any external heat. Noteworthy is the apparent greater reactivity of sepiolite *vs.* palygorskite in forging a stable complex with indigo. It was also observed that the heating time required for the dye in the palygorskite-indigo (at 150ºC) and sepiolite-indigo (120ºC) adducts to sufficiently react with the clay mineral may be reduced to as little as 2 h. The PXRD and relative transmittance FTIR spectra of the prepared palygorskite-indigo (2 wt.% indigo) and sepiolite-indigo (2 wt.% indigo) compounds were obtained and found to be in agreement with those previously reported by Kleber *et al.* (1967).

Chemical resistance of other indigo complexes

For comparison purposes, montmorillonite-indigo, silica-indigo and sand-indigo mixtures were produced but did not show any resistance to nitric acid before or after heating. Interestingly, a Na silicate-indigo compound prepared in the laboratory displayed all of the major chemical properties of Maya Blue after being heated at 150ºC for 20 h.

Sepiolite nitrogen adsorption-desorption isotherms

The nitrogen adsorption-desorption isotherms of purified sepiolite are shown in Figure 2. The curve may be classified as a general Type IV isotherm characteristic of a microporous material, with some inherent inter-particle mesoporosity. The insert in Figure 2, a magnification of the low-pressure region, reveals the definite presence of accessible micropores. The BET surface area was found to be 298±4 m^2/g. This measurement was confirmed by performing a congruent analysis using Argon (Ar) as the adsorbed gas, yielding a BET surface measurement of 284±3 m^2/g. T-plot data for purified sepiolite indicate a micropore area of 152 m^2/g, a corresponding micropore volume of 77 mm^3/g (Table 1), and an external surface area of 145 m^2/g. Estimation of the micropore volume was

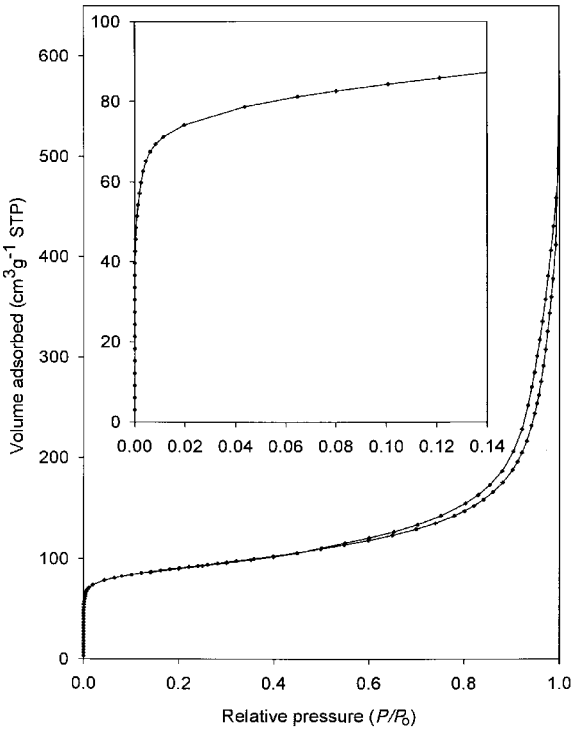

Figure 2. Nitrogen adsorption-desorption isotherms of purified sepiolite (SepSp-1) at −196ºC.

enabled through desorption of the internal zeolitic water molecules during degassing.

Sepiolite micropore volume

Figure 3 shows the low-pressure region of adsorptions for purified sepiolite (a), purified sepiolite heated at 120ºC for 20 h (c), and the corresponding sepiolite-indigo (2 wt.% indigo) preparations (b, d). It is striking that the microporous structure of sepiolite is preserved upon heating to 120ºC. The micropore area prior to heating was recorded as 152 m^2/g; the area after heating was 158 m^2/g (Table 1). It is evident that crushing sepiolite with indigo results in a significant decline in microporosity. Specifically, the micropore area decreased from 152 m^2/g in the pure sepiolite sample

Table 1. Micropore analysis of palygorskite-indigo and sepiolite-indigo.

Sample description	T-plot		Horvath-Kawazoe	
	Micropore area (m^2/g)	Micropore volume (mm^3/g)	Cumulative pore volume (mm^3/g)	Median pore diameter (Å)
Unheated pure palygorskite	93	47	89	6.1
Unheated, crushed 2% palygorskite-indigo	67	34	81	6.8
Pure palygorskite heated at 150ºC for 20 h	93	46	93	6.2
Crushed 2% palygorskite-indigo heated at 150ºC for 20 h	19	9	54	7.8
Unheated pure sepiolite	152	77	137	6.3
Unheated, crushed 2% sepiolite-indigo	113	57	83	7.0
Pure sepiolite heated at 120ºC for 20 h	158	80	132	6.3
Crushed 2% sepiolite-indigo heated at 120ºC for 20 h	61	30	82	7.5

https://doi.org/10.1346/CCMN.2003.0510308 Published online by Cambridge University Press

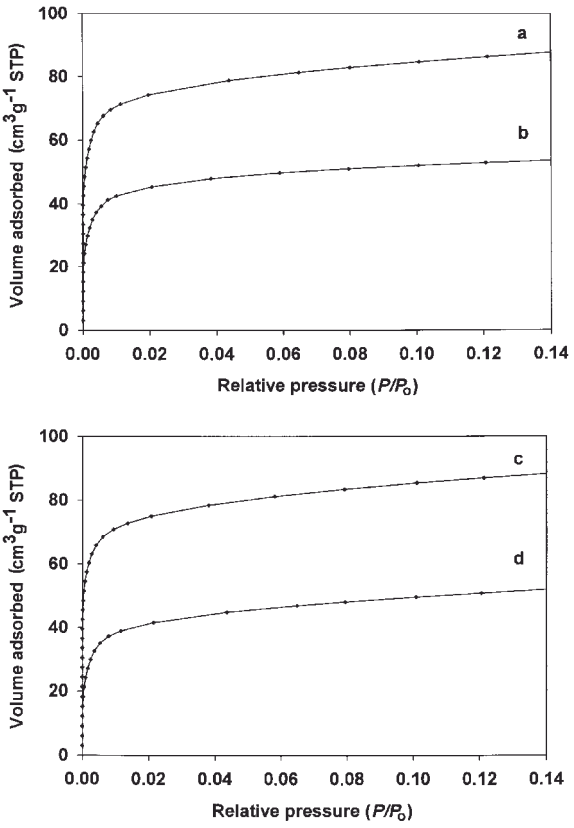

Figure 3. Nitrogen adsorption isotherms at −196ºC for (a) sepiolite, (b) crushed sepiolite-indigo (2 wt.% indigo), (c) sepiolite heated at 120ºC for 20 h, and (d) crushed sepiolite-indigo (2 wt.% indigo) heated at 120ºC for 20 h.

to 113 m^2/g in the unheated, crushed, sepiolite-indigo sample. Similarly, while the heated sepiolite sample was observed to have a micropore area of 158 m^2/g, the thermally treated sepiolite-indigo complex was characterized by a microporosity of 61 m^2/g. Consequently, the micropore volume of unheated sepiolite (77 mm^3/g) was larger than that of the unheated sepiolite-indigo complex (57 mm^3/g); the volume of the thermally treated samples dropped from 80 mm^3/g to 30 mm^3/g when indigo was present (Table 1). Similar trends were observed independently in a Horvath-Kawazoe (HK) analysis (Horvath and Kawazoe, 1983) where the cumulative pore-volume limit was specified as 20 Å (Table 1). The HK distribution of relative micropore dimensions revealed median pore diameters in the range 6.3–7.5 Å for the four sepiolite-based (unheated sepiolite, heated sepiolite, unheated sepiolite-indigo, and heated sepiolite-indigo) samples. These values are consistent with the theoretical dimensions of the rectangular tunnels found in the clay mineral (Jones and Galán, 1998). Pure sepiolite samples thermally treated at 150ºC for 20 h were also investigated and deemed equivalent to those heated at 120ºC for 20 h. The nitrogen adsorption data provide strong evidence that the micropores of sepiolite are partially blocked upon formation of the sepiolite-indigo adduct. Additionally, it appears as though the sepiolite pores which remain accessible after interaction with indigo retain their primary structure.

Palygorskite micropore volume

A similar gas-adsorption/desorption study was performed using palygorskite, and palygorskite-indigo adducts. The results of these experiments are also described in Table 1. Similar to pure sepiolite, pure palygorskite was observed to keep its microporosity following thermal treatment at 150ºC for 20 h. As for the unheated sepiolite-indigo complex, the unheated palygorskite-indigo complex also loses a significant amount of microporosity upon mixing with indigo. Moreover, the heated palygorskite-indigo complex loses most of its microporosity. It is ascertained that only a fraction of the total micropores remains unobstructed after formation of the palygorskite-indigo complex. The median pore diameters of the heated palygorskite-indigo complex are larger than that of pure palygorskite (7.8 Å *vs.* 6.1 Å).

Thermal analysis of indigo complexes

Since the structural characteristics of the sepiolite-indigo and palygorskite-indigo adducts are evidently temperature dependent, a TGA study of these complexes was performed. In the first series of thermal experiments, sepiolite and sepiolite-indigo (2 wt.% indigo), and palygorskite and palygorskite-indigo (2 wt.% indigo) samples were ramped to 120ºC and 150ºC, respectively, and maintained at these temperatures for 2 h. The findings of these investigations are described in Figures 4 (sepiolite-indigo) and 6 (palygorskite-indigo). In both the sepiolite-indigo and the palygorskite-indigo DTG curves, weight losses are apparent during the thermal escalation to the specified plateau temperatures. These weight losses, ~8.8% in sepiolite and 11.0% in palygorskite, are attributed to the loss of externally bound and zeolitic water. Endothermic peaks on both of the DTA plots confirm these water losses. When the plateau temperature was reached after 10 or 15 min (in palygorskite and sepiolite, respectively), no further major mass loss was observed. It may be assumed that all of the loosely bound water was lost at this point. The results of these studies, shown in Figures 4 and 6 (sepiolite-indigo and palygorskite-indigo, respectively), are essentially equivalent to the results of the corresponding blank experiments performed on purified sepiolite and palygorskite.

After being maintained at 120ºC (sepiolite-based samples) and 150ºC (palygorskite-based samples) for 2 h, the four aforementioned samples were cooled under air to room temperature over a period of 1 h. A standard TGA analysis to 1000ºC was then performed on the same samples using He gas. The results of these experiments are shown in Figures 5 and 7, for sepiolite and sepiolite-indigo, and palygorskite and palygorskite-indigo,

https://doi.org/10.1346/CCMN.2003.0510308 Published online by Cambridge University Press

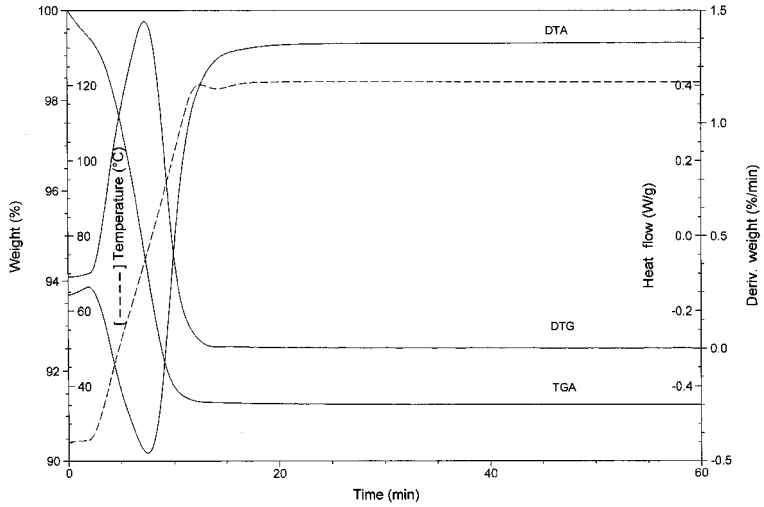

Figure 4. Thermal analysis (TGA, DTG, DTA) of crushed sepiolite-indigo (2 wt.% indigo) ramped to 120ºC and heated at this temperature for 2 h (only the first hour is shown); the temperature curve is illustrated with a broken line.

respectively. In all four cases, four major weight loss stages may be identified on the TGA curve. For sepiolite, the first weight loss of 0.8% occurs from room temperature to 100ºC and is attributed to loosely bound water; the second loss, of 3.3 wt.%, occurs between 100 and 300ºC and represents the first structural water. This is followed by a loss of 3.0% in the 300–600ºC ranges corresponding to the loss of the second structural water, and a loss of ~2.7% in the high-temperature region (600–900ºC) caused by dehydroxylation of the edge silanol and the structural Mg-OH groups. The TGA of the sepiolite-indigo complex is virtually identical with the exception of an additional peak at ~360ºC identified as indigo through comparison with the TGA curve of pure synthetic indigo which shows a weight loss of ~80% occurring at the same temperature due to decomposition. The results of the palygorskite/palygorskite-indigo experiment (Figure 7) mirror those of the sepiolite/sepiolite-indigo (Figure 5) investigation. Overall, the TGA results show that the global structure of sepiolite and palygorskite was maintained after heating in the presence of indigo. It was noteworthy that the temperature of decomposition of indigo in the adduct was nearly identical to that of the pure compound.

^{29}Si CP/MAS-NMR spectra

The ^{29}Si CP/MAS-NMR spectra of sepiolite and sepiolite heated at 120ºC for 20 h are shown in Figure 8, and are in agreement with those reported previously (Weir *et al.*, 2002). In the heated sample, the ^{29}Si CP/MAS-NMR signals of the center and the edge Si nuclei coincide at –97.0 ppm. The near-edge Si is represented by a chemical shift at –93.7 ppm. The corresponding

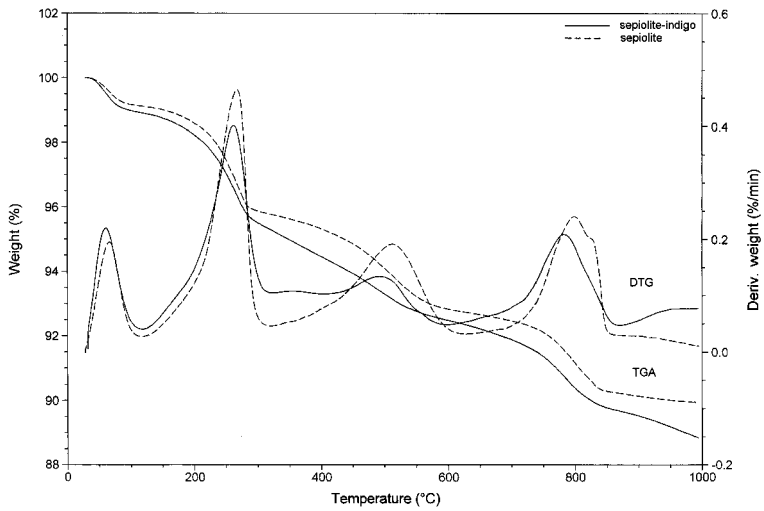

Figure 5. Thermal comparison (TGA, DTG) between crushed sepiolite-indigo (2 wt.% indigo) and pure sepiolite both preheated at 120ºC for 2 h and cooled to room temperature under air flow prior to analysis.

https://doi.org/10.1346/CCMN.2003.0510308 Published online by Cambridge University Press

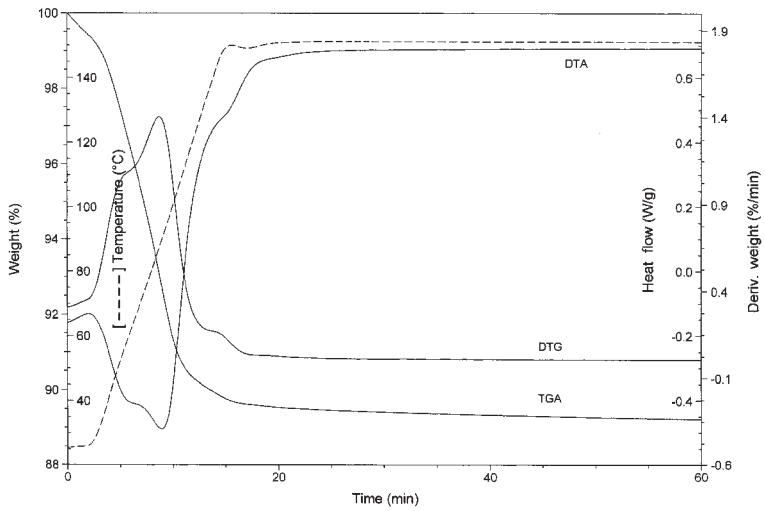

Figure 6. Thermal analysis (TGA, DTG, DTA) of crushed palygorskite-indigo (2 wt.% indigo) ramped to 150ºC and heated at this temperature for 2 h (only the first hour is shown); the temperature curve is illustrated with a broken line.

spectra recorded for the sepiolite-indigo (20 wt.% indigo) adduct (Figure 8c,d) confirm that the structure of sepiolite is maintained upon thermal treatment in the presence of indigo. This observation is in diametric contrast to that which is expected for an intercalated material. It was previously documented that upon exposure to acetone vapor, dehydrated sepiolite sequesters individual molecules of acetone in its microporous tunnels, resulting in the recovery of the original hydrated ^{29}Si CP/MAS-NMR spectrum (Weir *et al.*, 2000). A similar observation was reported after intercalation of pyridine (Kuang *et al.*, 2002). The ^{29}Si CP/MAS data indicate that indigo is not inserted into the nano-tunnels of sepiolite in the same fashion as smaller organic molecules such as acetone or pyridine.

^{13}C CP/MAS-NMR spectra

Figure 9 displays the ^{13}C CP/MAS-NMR spectrum of indigo (a), crushed sepiolite-indigo (2 wt.% indigo) (b), and crushed sepiolite-indigo (2 wt.% indigo) heated at 120ºC for 20 h (c). The broadness of the ^{13}C line spectrum of pure indigo may be accounted for by the presence of multiple crystallographic sites for each carbon in the indigo molecule (Gribova, 1955). Molecular variance such as this arises due to strong intermolecular associations, and aggregation between neighboring indigo molecules. It was confirmed through ^{13}C CP/MAS-NMR that heating pure indigo alone to 120 or 150ºC for 20 h does not cause any significant changes in the crystalline structure. From the spectrum of the unheated sepiolite-indigo adduct, it is clear that dramatic

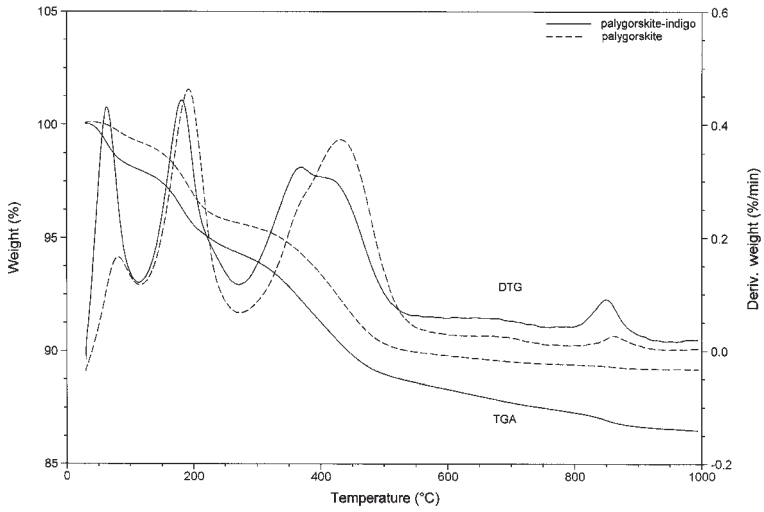

Figure 7. Thermal comparison (TGA, DTG) between crushed palygorskite-indigo (2 wt.% indigo) and pure palygorskite both preheated at 150ºC for 2 h and cooled to room temperature under air flow prior to analysis.

https://doi.org/10.1346/CCMN.2003.0510308 Published online by Cambridge University Press

changes occur in the ^{13}C CP/MAS-NMR spectrum of sepiolite-indigo after merely crushing the two together. Two species of indigo may be distinguished in this spectrum, one being unaffected pure indigo, and the other representing an altered state of the indigo molecules. In this spectrum, all of the ^{13}C signals narrow, a well defined series of peaks develops in 120.0–125.0 ppm range, and two translated peaks bearing chemical shifts of 191.1 ppm and 137.8 ppm are observed. The peak at 191.1 ppm is representative of the carbonyl group and the peak at 137.8 ppm maps to the C-7 and C-16 of the indigo molecule (see Figure 1). After thermal treatment of the mixture at 120ºC for 20 h, the original peaks of indigo vanish, and are replaced by eight well-resolved signals corresponding to the eight unique carbons of the reacted indigo molecules.

A sample of sepiolite-indigo with excess indigo was prepared (20 wt.% indigo), rinsed with nitric acid and characterized using ^{13}C CP/MAS-NMR in an identical manner; only the altered indigo species was observed. The narrowness of the signals in the sepiolite-indigo adduct spectrum indicates disaggregation of associated molecules, and a shift from crystallographic symmetry to molecular symmetry. The relatively small difference in chemical shifts between the ^{13}C NMR spectrum of pure indigo and that of the sepiolite-indigo adduct is in contrast to the change in chemical shifts observed after an organic molecule is incorporated in the nano-tunnels. For example, the resonance for the carbonyl group of acetone molecules undergoes a downfield shift in excess of 10.0 ppm upon incorporation into the nano-tunnels of sepiolite (Kuang *et al*., 2002). The chemical shift for the carbonyl group in the sepiolite-indigo adduct is translated a mere 1.6 ppm from that of pure indigo. These shifts are in good agreement with the proposed model below, where the carbonyl groups of indigo interact with edge silanol groups, not with the internal surfaces of the nano-tunnels.

A mirror ^{13}C CP/MAS-NMR study was performed using palygorskite as the base clay mineral. However, the spectrum acquired had a very low signal/noise ratio presumably due to the paramagnetic Fe in the clay mineral. The presence of Fe in close proximity to indigo was reported by Polette *et al*. (2002).

Model of indigo complexes

The ^{29}Si and ^{13}C CP/MAS-NMR results point to a monomolecular indigo coverage of the sepiolite surface. This interpretation is also in agreement with the TGA analysis. However, the textural study performed on palygorskite-indigo and sepiolite-indigo adducts indicates the loss of micropore accessibility upon formation of the clay-indigo complex. These results lead to a model where indigo molecules cover the openings of nano-tunnels, and are plausibly anchored by hydrogen bonds of their carbonyl and amino groups to silanol groups projected out from the edges of the tunnels.

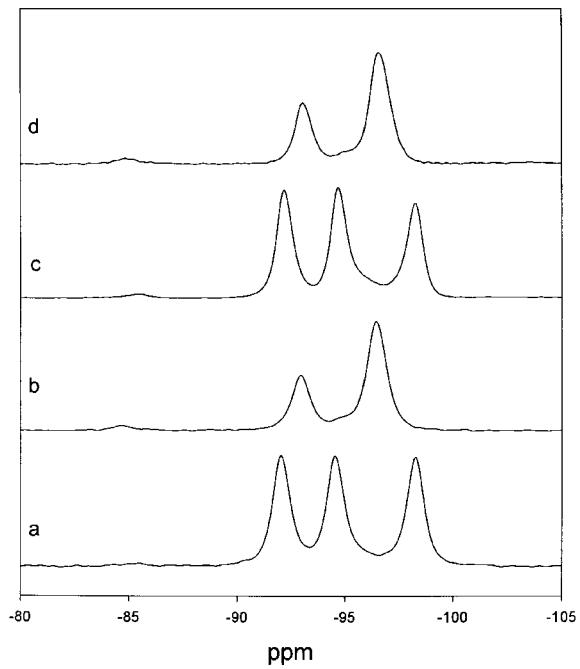

Figure 8. ^{29}Si CP/MAS-NMR spectra obtained at 25ºC of (a) unheated sepiolite, (b) sepiolite heated at 120ºC for 20 h, (c) crushed sepiolite-indigo (20 wt.% indigo), and (d) crushed sepiolite-indigo (20 wt.% indigo) heated at 120ºC for 20 h.

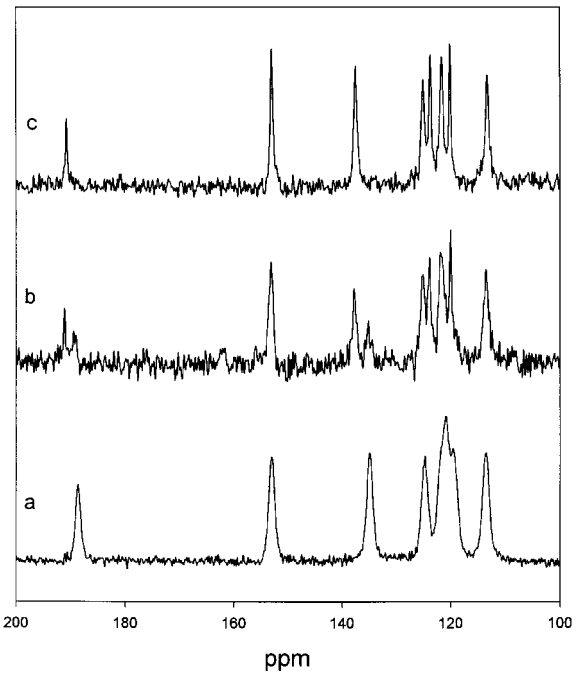

Figure 9. ^{13}C CP/MAS-NMR spectra obtained at 25ºC of (a) synthetic indigo, (b) crushed sepiolite-indigo (2 wt.% indigo), and (c) crushed sepiolite-indigo (2 wt.% indigo) heated at 120ºC for 20 h.

https://doi.org/10.1346/CCMN.2003.0510308 Published online by Cambridge University Press

CONCLUSIONS

Textural analysis indicates that the micropores of sepiolite and palygorskite become partially inaccessible after thermal treatment in the presence of indigo. The TGA and DTG curves of the sepiolite-indigo and palygorskite-indigo adducts obtained are very similar to their pure clay mineral counterparts except for an additional weight loss at ~360ºC corresponding to indigo. The ^{29}Si CP/MAS-NMR spectra of the heated sepiolite-indigo adduct is essentially equivalent to that of pure dehydrated sepiolite. The ^{13}C CP/MAS-NMR spectrum of the heated sepiolite-indigo adduct is composed of a well defined series of peaks in the 120.0–125.0 ppm range, as well as two shifted peaks corresponding to the carbonyl group and the C-7 (C-16) of the indigo molecule. The narrowness of the signals in the ^{13}C spectrum of the sepiolite-indigo adduct is indicative of a transition from crystallographic symmetry to molecular symmetry, corresponding also to a transition from an aggregated state to a molecular state. The model proposed is one where indigo molecules covering the openings of nano-tunnels are anchored by hydrogen bonds of their carbonyl and amino groups to silanol groups bordering the micropores.

ACKNOWLEDGMENTS

The Natural Science and Engineering Research Council of Canada (NSERC) is gratefully acknowledged for a research grant to CD. The University of Ottawa is thanked for an Undergraduate Research Scholarship to BH. Ms Elizabeth Cross is noted for her help with the bibliographic research.

REFERENCES

Ahlrichs, J.L., Serna, C. and Serratosa, J.M. (1975) Structural hydroxyls in sepiolite. *Clays and Clay Minerals*, **23**, 119–124.

Brindley, G.W. (1959) X-ray and electron diffraction data for sepiolite. *American Mineralogist,* **44**, 495–500.

Cooksey, C.J. and Dronsfield, A.T. (2002) Adolf von Baeyer and the indigo molecule. *Dyes in History and Archaeology*, **18,** 13–19.

Gettens, R.J. (1962) Maya blue: an unsolved problem in ancient pigments. *American Antiquity*, **27**, 557–564.

Gettens, R.J. and Stout, G.L. (1946) *Painting Materials: A Short Encyclopedia*. D. Van Nostrand, New York, pp. 130–131.

Gordon, P.F. and Gregory, P. (1983) Indigoid Dyes. Pp. 208–211 in: *Organic Chemistry in Colour*. Springer-Verlag, Berlin.

Gribova, E.A. (1955) X-ray study of indigo and thioindigo. *L. Ya. Karpov Physical Chemistry Institute: Doklady Akademii Nauk SSSR*, **102**, 279–81.

Horvath, G. and Kawazoe, K. (1983) Method for the calculation of effective pore size distribution in molecular sieve carbon. *Journal of Chemical Engineering of Japan*, **16**, 470–475.

Jones, B.F. and Galán, E. (1998) Sepiolite and palygorskite. Pp. 631–674 in: *Hydrous Phyllosilicates* (S.W. Bailey, editor). Reviews in Mineralogy, **19**. Mineralogical Society of America, Washington, D.C.

Jose-Yacaman, M., Rendon, L., Arenas, J. and Puche, M.C.S. (1996) Maya blue paint: an ancient nanostructured material. *Science*, **273**, 223–225.

Kleber, R., Masschelein-Kleiner, L. and Thissen, J. (1967) Study and identification of Maya blue. *Studies in Conservation*, **12**, 41–56.

Kuang, W., Hubbard, B., Moser, A., Facey, G.A. and Detellier, C. (2002) Organo-sepiolite and palygorskite nanocomposites. *Proceedings of the 5th International Conference on Solid State Chemistry*, Bratislava, Slovak Republic**.**

Le Van Mao, R., Rutinduka, E., Detellier, C., Gougay, P., Hascoet, V., Tavakoliyan, S., Hoa, S.V. and Matsuura, T. (1999) Mechanical and pore characteristics of zeolite composite membranes. *Journal of Materials Chemistry*, **9**, 783–788.

Merwin, H.E. (1931) In: *The Temple of the Warriors at Chichen Itza* (E.H. Morris, J. Charlot and A.A. Morris, editors). Carnegie Institution of Washington, Washington, D.C., publ. 406.

Myriam, M., Suarez, M. and Martin-Pozas, J.M. (1998) Structural and textural modifications of palygorskite and sepiolite under acid treatment. *Clays and Clay Minerals*, **46**, 225–231.

Pedro, G. (1972) Report of the AIPEA Nomenclature Committee. *AIPEA Newsletter*, **4**, 3–4.

Polette, L.A., Meitzner, G., Jose-Yacaman, M. and Chianelli, R.R. (2002) Maya blue: application of XAS and HRTEM to materials science in art and archaeology. *Microchemical Journal*, **71**, 167–174.

Ruiz-Hitzky, E. (2001) Molecular access to intracrystalline tunnels of sepiolite. *Journal of Materials Chemistry*, **11**, 86–91.

Serna, C. and van Scoyoc, G.E. (1979) Infrared study of sepiolite and palygorskite surfaces. Pp. 197–206 in: *Proceedings of the International Clay Conference, Oxford, 1978* (M.M. Mortland and V.C. Farmer, editors). Elsevier, Amsterdam.

Shepard, A. (1962) Maya blue: alternative hypotheses. *American Antiquity,* **27**, 565–566.

Tagle, A., Paschinger, H., Richard, H. and Infante, G. (1990) Maya blue: its presence in Cuban colonial wall paintings. *Studies in Conservation*, **35**, 156–159.

Van Olphen, H. (1966) Maya Blue: a clay mineral-organic pigment? *Science*, **154**, 645–646.

Wang, Q.K., Matsuura, T., Feng, C.Y., Weir, M.R., Detellier, C., Rutinduka, E. and Le Van Mao, R. (2001) The sepiolite membrane for ultrafiltration. *Journal of Membrane Science*, **184**, 153–163.

Weir, M.R., Facey, G.A. and Detellier, C. (2000) ^{1}H, ^{2}H and ^{29}Si solid state NMR study of guest acetone molecules occupying the zeolitic channels of partially dehydrated sepiolite clay. *Studies in Surface Science and Catalysis,* **129**, 551–558.

Weir, M.R., Rutinduka, E., Detellier, C., Feng, C.Y., Wang, Q., Matsuura, T. and Le Van Mao, R. (2001) Fabrication, characterization and preliminary testing of all-inorganic ultrafiltration membranes composed entirely of a naturally occurring sepiolite clay mineral. *Journal of Membrane Science*, **182**, 41–50.

Weir, M.R., Kuang, W., Facey, G.A. and Detellier, C. (2002) Solid state nuclear magnetic resonance study of sepiolite and partially dehydrated sepiolite. *Clays and Clay Minerals,* **50**, 240–247.

(*Received 13 September 2002; revised 3 February 2003; Ms. 716; A.E. William F. Jaynes*)